Spectral functions in an exactly solvable self-bound A-body system

D. Van Neck, S. Rombouts, and S. Verdonck
Laboratory of Theoretical Physics, Ghent University, Proeftuinstraat 86, B-9000 Gent, Belgium
(Received 30 August 2005; published 29 November 2005)

We consider an exactly solvable Hamiltonian for bosons in one-dimension interacting through zero-range attractive forces, and construct a complete basis of its A-particle eigenstates. The structure of the single-particle spectral function in the removal domain is investigated, by taking the overlap of the A-particle ground state with the various excited states of the $(A-1)$ system. In particular we study the contribution to the spectral function of the different break-up channels in the $A-1$ continuum, and compare the results to general statements available in the literature. It is shown that the asymptotic behavior in coordinate space does not agree with conventional assumptions. The relation to recent $(e,e'p)$ experiments at large values of missing energy and momentum is pointed out.

DOI: 10.1103/PhysRevC.72.054318 PACS number(s): 24.10.Cn, 21.60.−n, 25.30.Fj

I. INTRODUCTION

The single-particle spectral function $S(k,E)$ can be defined as the probability for ending up in an eigenstate of the $(A\pm1)$-particle system at energy E, when a particle with momentum k is added to, or removed from, the correlated A-particle ground state. It is a central concept in the Green's function description of interacting many-body systems [1,2]. Apart from this theoretical status, it is also a quantity that is experimentally accessible, and in particular one-particle knock-out reactions are mostly analyzed in terms of the removal spectral function.

During the 90s, electron-induced $(e,e'p)$ (proton knock-out) reactions have provided a detailed mapping of the spectral function for complex nuclei in the proton removal region [3–5]. However, in most cases only the region of small nucleon momenta and removal energies was probed. In this energy-momentum region one expects the spectral function of a normal quantum system to be dominated by quasiparticle excitations.

Only recently has it become feasible to probe the spectral function away from the quasiparticle peak, at much larger values of missing momentum and missing energy [6–8]. In this kinematical region one may hope that the (one-body part of the) cross section is sensitive to the nonquasiparticle "background" of the spectral function. This would be important, as the background is closely related to the nature and strength of the NN interaction at short distances [9]. More generally, it would be highly interesting to have direct experimental corroboration of the intuitive nonrelativistic picture, where the nuclear spectral function is separated into quenched quasiparticle excitations (with nucleons moving in mean-field-like orbitals), and into a background or correlation part containing nucleons moving with much larger velocities [9–13].

The $(e,e'p)$ experiments at large missing energy are performed well beyond the threshold for two-nucleon emission. Although the shape of the overlap function is well-known for the case of overlaps with bound $(A-1)$ states, it is not immediately clear what is the nature of the overlap function between an unbound $A-1$ nucleon state, with one or more nucleons in the continuum, and the ground state of the target nucleus. In this paper we try to address this issue by considering an exactly solvable model.

The model we discuss involves a general number of spinless bosons moving in one dimension and interacting through attractive delta-function potentials. It has been used before to investigate general features of finite, self-bound many-body systems. Earlier studies focused on properties of the ground state, such as the comparison between the exact density, elastic form factor, and momentum distribution with their mean-field (Hartree-Bose) approximations [14–16]. More recently the full one-body density matrix (OBDM) was obtained for this model [17,18], and a study was made of the natural orbitals and the overlap function between the A and $A-1$ ground states. It was shown that such bound-state overlap functions can be obtained from the OBDM also in a more general setting [19,20].

It is not immediately obvious that the simple attractive delta-potential can be relevant for the properties of real systems like nuclei. The nucleon-nucleon interaction is complicated and has, in addition to the attractive components, a strong short-range repulsion. In fact it is the latter component that is mainly responsible for the high-momentum components in the nuclear wave function. Nevertheless, the present model is perfectly adequate to study the most general features related to self-bound systems, such as the ultimate asymptotic behavior of the momentum distribution. It can be shown (see, e.g., Ref. [15]) that for a nonsingular local interaction $v(r)$ the momentum distribution $n(k)$ behaves asymptotically as $[v(k)/k^2]^2$, where $v(k)$ is the Fourier transformed (FT) interaction. The large-momentum behavior is insensitive to the sign of v, and is governed by the fastest variations in $v(r)$. Physically, of course, this is usually the repulsive core at short distances. The present delta-interaction is extremely short-range and presents some kind of limit situation: the FT is a constant, whereas any other nonsingular interaction would eventually die out in momentum space.

In the present paper we extend the study of Ref. [17], by constructing a complete set of A-particle eigenstates for this system and investigating the single-particle removal spectral function. In particular we pay attention to the contribution

of unbound $A-1$ states with one or more particles in the continuum, and examine the properties of the corresponding overlap functions. Such a study in an exactly solvable model is useful in the sense that one can check general assumptions made in more realistic cases; it will be shown, e.g., that the asymptotic behavior of continuum $A-1$ overlap functions assumed in many articles is incorrect.

Another interesting point that can be addressed more fully in an exactly solvable model, is the decomposition of the OBDM (which receives contributions from all $A-1$ eigenstates) into quasiparticle and correlation parts, and the latter's signature in the momentum distribution and (coordinate space) density. While the high-momentum components induced by the correlation part are quite similar for the finite and infinite system, the signature in coordinate space is typical for a finite system. For the present model this was studied in Ref. [17]; it was found that the correlation contribution to the density is localized in the center and is of shorter range than the contributions from the quasiparticle excitations. The same features are present in detailed calculations for finite nuclei [19,21,22]. It was shown quite recently [23], by a comparison of $(e,e'p)$ results with the total charge density obtained from elastic electron scattering, that the experimental data can be consistently analyzed in terms of such quasiparticle and correlation densities. Interestingly, the authors of Ref. [23] were also able to provide a natural explanation for the discrepancy in the $(e,e'p)$ spectroscopic factors obtained in low-q and high-q experiments [24].

We learned recently that excited-state wave functions for the present model have already been considered in Ref. [25]. However, the interest there was in assessing the validity of symmetry-breaking mean-field descriptions of unconfined Bose-Einstein condensates, and properties of the spectral function for finite systems were not investigated.

II. EXACT MANY-BODY EIGENSTATES

A. Hamiltonian

The model Hamiltonian H involves A spinless bosons in one dimension, interacting with attractive δ-function potentials,

$$H_A = -\frac{1}{2m}\sum_{i=1}^{A}\frac{\partial^2}{\partial x_i^2} - g\sum_{i<j=1}^{A}\delta(x_i - x_j), \tag{1}$$

where $g>0$ and in units $\hbar = 1$.

For $A \geqslant 2$ there is one bound state with energy

$$E_{0(A)} = -\frac{\lambda^2}{6m}A(A^2-1), \tag{2}$$

where $\lambda = mg/2$. The intrinsic wave function of the ground state reads

$$\Psi_{0(A)}(x_1,\ldots,x_A) = C_A \exp\left(-\lambda\sum_{i<j=1}^{A}|x_i - x_j|\right), \tag{3}$$

with the normalization constant C_A given by $C_A = [(2\lambda)^{A-1}(A-1)!/A]^{1/2}$. We refer to Ref. [26] for our normalization conventions concerning the intrinsic (translationally invariant) eigenstates of self-bound systems.

B. A-particle eigenstates

The construction of the exact eigenstates proceeds using techniques related to the Bethe ansatz. It is quite analogous to the construction in Ref. [27] for the case of the repulsive δ-potential, except that for the analysis of the thermodynamic properties of the one-dimensional Bose gas in Ref. [27] periodic boundary conditions on a finite x-interval were imposed, whereas in the present treatment the position x is unrestricted and the particle number A is kept fixed. Moreover, additional complications arise because of the presence of a bound state for the attractive δ-potential.

For A particles there are $A!$ possible orderings of the positions, $x_{\pi(1)} \geqslant x_{\pi(2)} \ldots \geqslant x_{\pi(A)}$, where π is a permutation of the particle labels. Since an A-boson wave function is symmetrical,

$$\Psi_{(A)}(x_{\pi(1)}, x_{\pi(2)}, \ldots, x_{\pi(A)}) = \Psi_{(A)}(x_1, x_2, \ldots, x_A), \tag{4}$$

it is fully determined by its values $\Psi^{\mathrm{SO}}_{(A)}(x_1,\ldots,x_A)$ in e.g., the "standard" ordering $x_1 > x_2 > \cdots > x_A$.

Within any fixed ordering, the interaction terms in Eq. (1) are inconsequential, and the wave function must be of exponential type (or a sum of exponentials). The $\delta(x_i - x_j)$ interaction terms come into play when crossing between different orderings occurs and must be canceled by corresponding δ-terms in the kinetic term, originating from discontinuities in the normal derivatives when crossing an $x_i = x_j$ boundary. The precise cusp condition which ensures such a cancellation is

$$\lim_{x_i \overset{>}{\to} x_j}\left[2\lambda + \left(\frac{\partial}{\partial x_i} - \frac{\partial}{\partial x_j}\right)\right]\Psi_{(A)}(x_1, x_2, \ldots, x_A) = 0. \tag{5}$$

It is shown in the Appendix that for an arbitrary set of complex $(e_1, e_2, \ldots, e_A)$ the exponential-type function

$$\Psi^{\mathrm{SO}}_{(A)}(x_1, x_2, \ldots, x_A) = \sum_{\pi} W_\pi \exp\left(\sum_{i=1}^{A} e_{\pi(i)}x_i\right), \tag{6}$$

where the summation runs over all permutations π, obeys the cusp conditions in Eq. (5) and hence is an eigenfunction of the Hamiltonian in Eq. (1), provided the coefficients W_π are chosen as

$$W_\pi = \mathrm{sign}(\pi)\prod_{i<j=1}^{A}(2\lambda - e_{\pi(i)} + e_{\pi(j)}). \tag{7}$$

Here $\mathrm{sign}(\pi)$ refers to the odd or even character of the permutation π.

Not all choices of the e_i, however, lead to an acceptable physical eigenstate. Firstly, translational invariance of the wave function implies that $\sum_{i=1}^{A} e_i = 0$. Secondly, the condition that $\Psi_{(A)}$ should not be exponentially increasing at infinity severely restricts the possibilities for the real parts of the e_i. This reflects whether one or more bound clusters are present in the asymptotic behavior of the wave function.

We use the asymptotic cluster structure to classify the different continuum channels for the eigenstates. If $[n_1 n_2 \ldots n_N]$

is a partition of A, i.e., $1 \leqslant n_\alpha \leqslant A$ and $\sum_{\alpha=1}^{N} n_\alpha = A$, then this specifies N bound clusters, containing, respectively, particles $(1, \ldots n_1)$, $(n_1+1, \ldots, n_1+n_2)$, etc. In a more compact notation, cluster α contains particles $(N_\alpha+1, \ldots, N_\alpha+n_\alpha)$, where $N_\alpha = \sum_{\beta=1}^{\alpha-1} n_\beta$.

In the standard ordering we may consider the regime where the distance between the c.m. (center of mass) coordinates of the different clusters is taken to infinity, while the relative coordinates within each cluster remain finite. In this regime, the distance $|x_i - x_j|$ between any two particles not belonging to the same cluster becomes very large. A valid asymptotic behavior for an intrinsic A-particle eigenstate $\Psi^{\rm SO}_{(A)}$ of Eq. (1) is then given by the product of N bound eigenstates of the form (3), describing the internal motion within each cluster, and $N-1$ plane-wave states for the motion of the clusters reative to each other. The latter motion can be fully specified by $N-1$ (real) numbers k_α $(\alpha = 2, \ldots, N)$, denoting, e.g., the momentum of the c.m. X_α of cluster α with respect to the total c.m. $\tilde{X}_\alpha$ of the preceding clusters $1, \ldots, \alpha-1$. The asymptotic behavior as specified above by the partition $[n_1 n_2 \ldots n_N]$ and momenta k_α, then reads

$$\Psi^{\rm SO}_{(A)} \to \left[\prod_{\alpha=1}^{N} \exp\left(-\lambda \sum_{i<j=1}^{n_\alpha} |x_{N_\alpha+i} - x_{N_\alpha+j}|\right)\right] \times \left[\prod_{\alpha=2}^{N} \exp\left(\mathrm{i}k_\alpha (X_\alpha - \tilde{X}_\alpha)\right)\right], \tag{8}$$

where $X_\alpha = (\sum_{i=1}^{n_\alpha} x_{N_\alpha+i})/n_\alpha$, and $\tilde{X}_\alpha = (\sum_{\beta=1}^{\alpha-1} \sum_{i=1}^{n_\beta} x_{N_\beta+i})/N_\alpha$. Since we assume standard ordering of the positions x_i, this can be rewritten simply as (for notational convenience we also introduce $k_1 = 0$),

$$\Psi^{\rm SO}_{(A)} \to \exp\left\{\sum_{\alpha=1}^{N}\sum_{j=1}^{n_\alpha}\left[-\lambda(n_\alpha - 2j + 1) + \mathrm{i}\left(\frac{k_\alpha}{n_\alpha} - \sum_{\beta=\alpha+1}^{N} \frac{k_\beta}{N_\beta}\right)\right] x_{N_\alpha+j}\right\} \tag{9}$$

$$= \exp\left(\sum_{i=1}^{A} e_i x_i\right). \tag{10}$$

We now show that inserting the set of exponents e_i defined in Eqs. (9) and (10) into Eqs. (6) and (7) leads to a physical eigenstate, with asymptotic behavior determined by Eq. (8). Obviously, $\sum_{i=1}^{A} e_i = 0$ since Eq. (8) is expressed in terms of relative coordinates. For the second condition we note that Eq. (7) implies $W_\pi = 0$ *unless* the inverse permutation π^{-1} keeps the order of the labels $N_\alpha + 1 < N_\alpha + 2 < \cdots < N_\alpha + n_\alpha$ belonging to the same cluster α, i.e., unless $\pi^{-1}(N_\alpha+1) < \pi^{-1}(N_\alpha+2) < \cdots < \pi^{-1}(N_\alpha+n_\alpha)$. Suppose otherwise, then $\pi^{-1}(N_\alpha+i) > \pi^{-1}(N_\alpha+i+1)$ for two consecutive labels in the cluster α, and the product in Eq. (7) would contain the factor $2\lambda - (e_{N_\alpha+i} - e_{N_\alpha+i+1}) = 0$. Stated differently, a term in Eq. (6) with nonzero coefficient W_π has within each cluster the positions $x_{\pi^{-1}(N_\alpha+i)}$ in standard order,

$$x_{\pi^{-1}(N_\alpha+1)} > x_{\pi^{-1}(N_\alpha+2)} > \cdots > x_{\pi^{-1}(N_\alpha+n_\alpha)}. \tag{11}$$

As a consequence, all terms appearing in the wave function (6) have an exponent with negative real part,

$$\Re\left(\sum_{i=1}^{A} e_{\pi(i)} x_i\right) = \Re\left(\sum_{i=1}^{A} e_i x_{\pi^{-1}(i)}\right) = -\lambda \sum_{\alpha=1}^{N}\sum_{i<j=1}^{n_\alpha} \left|x_{\pi^{-1}(N_\alpha+i)} - x_{\pi^{-1}(N_\alpha+j)}\right| \leqslant 0, \tag{12}$$

and qualify as physical eigenstates. Note that the number of permutations keeping the order in each cluster [i.e., obeying the inequalities (11)] is given by $A!/(n_1! \ldots n_N!)$, as expected from the symmetry properties of Eq. (8).

It still has to be shown that the asymptotic behavior is really given by Eq. (8), or equivalently, that the term in Eq. (6) corresponding to the unit permutation (the identity) is asymptotically dominating. From Eq. (12) it follows that the dominating terms in Eq. (6) are the ones where the image under π^{-1} of each cluster is itself a cluster. Otherwise, the sum in Eq. (12) would contain the distance $|x_{\pi^{-1}(N_\alpha+i)} - x_{\pi^{-1}(N_\alpha+j)}|$ between particles not belonging to the same cluster, and such a term in Eq. (6) would be exponentially damped in the asymptotic regime. Moreover, the mapping under π^{-1} of a cluster into a cluster must conserve the order, otherwise the permutation would have a zero coefficient W_π. In consequence, for a partition with no equivalent clusters (containing the same number of particles) the unit permutation is the only one that leads to a dominating term in the sum (6), and the asymptotic behavior of Eq. (8) follows. Equivalent clusters can of course still be interchanged in the asymptotic regime, and the corresponding dominating terms in Eq. (6) are generated by the permutations which map clusters into equivalent ones and are order conserving.

We have thus succeeded in constructing all intrinsic physical eigenstates of the model Hamiltonian (1). The A-particle eigenstates are labeled by their asymptotic behavior, in terms of a partition $[P] = [n_1 \ldots n_N]$ of A into N clusters, and a set of relative momenta $k_2, \ldots, k_N$ between the clusters. Including correct normalization factors we have, for $x_1 > \cdots > x_A$,

$$\Psi_{[P]\mathbf{K}}(\mathbf{x}) \equiv \Psi_{[P];k_2 \ldots k_N}(x_1, \ldots, x_A) = \frac{\mathcal{C}_{[P]}}{|W_1|} \times \sum_{\pi} W_\pi \exp\left(\sum_{i=1}^{A} e_{\pi(i)} x_i\right), \tag{13}$$

where the e_i follow from Eqs. (9) and (10), the permutation coefficients W_π from Eq. (7), and W_1 refers to the unit permutation. The factor $\mathcal{C}_{[P]}$ reads

$$\mathcal{C}_{[P]} = C_{n_1} \ldots C_{n_N} \left(\frac{n_1! \ldots n_N!}{A!(2\pi)^{N-1}}\right)^{1/2}, \tag{14}$$

TABLE I. Distribution of the strength of a normalized test function (see text) over the exact eigenstates. The results for particle number $A = 2, 3, 4, 5$ are classified according to the different partitions, corresponding to different break-up channels.

$A = 2$	[2] 0.8889	[1^2] 0.1111					
$A = 3$	[3] 0.7901	[21] 0.1804	[1^3] 0.0295				
$A = 4$	[4] 0.7023	[31] 0.2039	[21^2] 0.0555	[2^2] 0.0307	[1^4] 0.0076		
$A = 5$	[5] 0.6243	[41] 0.2291	[31^2] 0.0617	[32] 0.0458	[$2^2 1$] 0.0203	[21^3] 0.0170	[1^4] 0.0019

in terms of the bound-state normalization C_n in Eq. (3). The wave functions are now normalized as

$$\int dx_1 \dots dx_A \delta(R_A) \Psi^*_{[P];k_2 \dots k_N}(x_1, \dots, x_A) \times \Psi_{[P'];k'_2 \dots k'_{N'}}(x_1, \dots, x_A) = \delta_{P,P'} \prod_{\alpha=2}^{N} \delta(k_\alpha - k'_\alpha), \quad (15)$$

where $R_A = \sum_{i=1}^{A} x_i/A$ is the total c.m. coordinate.

The complete set of eigenstates is then generated by summing over all possible partitions and integrating all relative momenta over the entire range $[-\infty, +\infty]$. If equivalent clusters are present we must correct for double-counting of the relative momenta, e.g., for a partition $[P] = [nnnmm \dots] = [n^3 m^2 \dots]$ we must divide by $D_{[P]} = 3!2! \dots$. For a numerical check of the completeness we calculated the overlap of the eigenstates (13) with normalized test functions of the form $\Psi \sim \exp(-\lambda' \sum_{i<j=1}^{A} |x_i - x_j|)$, with $\lambda \neq \lambda'$ (i.e., the ground state of the system with a different coupling strength). The sum rule

$$1 = \sum_P \frac{1}{D_{[P]}} \int dk_2 \dots dk_N \Big| \int dx_1 \dots dx_A \delta(R_A) \times \Psi^*(x_1, \dots, x_A) \Psi_{[P]\mathbf{K}}(x_1, \dots, x_A) \Big|^2 \quad (16)$$

was seen to be fulfilled. As an example we list in Table I, for $A = 2$–5 and $\lambda' = 2\lambda$, the contributions to the sum rule (16) from the ground state and from the different break-up channels in the continuum (after integration over relative momenta). Note that, here and in the following, the multidimensional coordinate-space integrations are all of exponential type, and are done algebraically.

It should be noted that the eigenstates of Eq. (13) do not necessarily have good parity, but obey

$$\Psi_{[P]\mathbf{K}}(-\mathbf{x}) = s_{[P]}(\Psi_{[P]\mathbf{K}}(\mathbf{x}))^* = s_{[P]}(\Psi_{[P]-\mathbf{K}}(\mathbf{x})), \quad (17)$$

where $s_{[P]} = (-1)^{(A^2 - \sum_\alpha n_\alpha^2)/2}$ contains the signature of the permutations needed to reverse the order in each cluster of the partition $[P]$. Using Eq. (17) it is possible to introduce states of good parity and a restricted set of relative momenta $\mathbf{K}$. However, the parity quantum number is never relevant for the following, and we continue to work with states labeled solely by $[P]$ and $\mathbf{K}$.

Finally, the energy of the eigenstates of Eq. (13) can be evaluated as

$$E_{[P];k_2 \dots k_N} = -\frac{1}{2m} \sum_{i=1}^{A} e_i^2 = \sum_{\alpha=2}^{N} \left(\frac{1}{n_\alpha} + \frac{1}{N_\alpha} \right) \frac{k_\alpha^2}{2m} - \sum_{\alpha=1}^{N} \frac{\lambda^2}{6m} n_\alpha \left(n_\alpha^2 - 1 \right) = T_{[P];k_2 \dots k_N} + E^{\mathrm{tr}}_{[P]}, \quad (18)$$

where the first term $T_{[P];k_\alpha}$ represents the kinetic energy of the relative motion of the clusters and includes the correct reduced mass, and the second term $E^{\mathrm{tr}}_{[P]}$ is the threshold energy of this break-up channel, containing the binding energies of the clusters.

III. SPECTRAL FUNCTION FOR REMOVAL OF A PARTICLE

A. Overlap functions in coordinate space

The (single-particle) overlap function $\psi_{\nu(A-1)}(x)$ between the A-particle ground state $\Psi_{0(A)}$ and an $(A-1)$-particle eigenstate $\Psi_{\nu(A-1)}$ is defined as [26]

$$\psi_{\nu(A-1)}(x_A) = \sqrt{A} \int dx_1 \dots dx_{A-1} \delta(R_{A-1}) \Psi^*_{\nu(A-1)} \times (x_1, \dots, x_{A-1}) \Psi_{0(A)}(x_1, \dots, x_{A-1}, x_A). \quad (19)$$

Even for $(A-1)$ eigenstates in the continuum, the overlap function is normalizable, and the spectroscopic factors $S_{\nu(A-1)}$,

$$S_{\nu(A-1)} = \int dx |\psi_{\nu(A-1)}|^2, \quad (20)$$

obey the sumrule $\sum_\nu S_{\nu(A-1)} = A$.

In the present model all many-particle eigenstates are known exactly [see Eq. (13)]. The overlap integrals are all of exponential type, and with suitable bookkeeping the overlap functions are also known algebraically. The simplest case is for $A = 3$, where there are only two types of removal overlap functions with the two-particle system,

$$\psi_{[2]}(x) = 2\sqrt{2\lambda} \left(\mathrm{e}^{-2\lambda|x|} - \tfrac{1}{3} \mathrm{e}^{-6\lambda|x|} \right), \quad (21)$$

$$\psi_{[11]k}(x) = 4\lambda^2 \sqrt{\frac{2}{\pi}} \frac{\mathrm{e}^{-4\lambda|x|} \cos(2k|x| - \delta_k)}{\sqrt{(k^2 + \lambda^2)(k^2 + 4\lambda^2)}} \quad \left(\tan \delta_k = \frac{2\lambda}{k} \right). \quad (22)$$

Of particular importance is the large-distance ($|x| \to +\infty$) behavior of the overlap functions. In the literature one conventionally finds (see, e.g., Ref. [28,29]) the normal behavior

$$\psi_{\nu(A-1)}(x) \sim \mathrm{e}^{-\kappa_\nu |x|}, \kappa_\nu = \sqrt{2m\left(\frac{A-1}{A}\right)[E_{\nu(A-1)} - E_{0(A)}]}, \tag{23}$$

where the inverse decay length κ_ν is governed by the separation energy $[E_{\nu(A-1)} - E_{0(A)}]$. This result, while not rigorously proven, is generally accepted for single-particle overlaps to discrete (bound) $A-1$ states. The overlap function (21) with the bound two-particle state obeys this rule; also for general A, the overlap function between the A and $A-1$ ground-state has an asymptotic behavior with inverse decay length $\kappa_{[A-1]} = (A-1)\lambda$, in agreement with Eqs. (2) and (23).

It is commonly assumed (see, e.g., Ref. [28]) that the standard behavior of the overlap in Eq. (23) can be extended to the case of unbound $(A-1)$ states, where $E_{\nu(A-1)}$ is a continuous variable. The overlap functions (22) with the unbound two-particle states, however, do not follow the standard rule (23), according to which the overlap functions should be of increasingly shorter range as $E_{[11]}$ grows. In contrast, the exact overlap function in Eq. (22) has a damped oscillatory character, with the exponential damping having a fixed decay length, and an increasing energy giving rise to faster oscillations. For larger A, where more decay channels are possible, we always find the same behavior, i.e., for an N-cluster partition $[P]$ of $A-1$:

$$\psi_{[P]k_2,..k_N}(x) \sim \mathrm{e}^{-\kappa_{[P]}|x|} \times (\text{oscillatory terms}), \tag{24}$$

with the inverse decay length $\kappa_{[P]}$ determined by the partition and independent of the momenta between the asymptotic clusters. In fact, numerically we find

$$\kappa_{[P]} = (A-n)(A-1)\lambda, \tag{25}$$

with n the largest (most deeply bound) cluster appearing in the partition $[P]$ of the $(A-1)$ system, though we are unable to relate this in a simple way to the separation energies of the clusters. Such deviations from the standard rule (23) were not taken into account in previous work by one of the present authors [30]. However, the general results in Ref. [30] only need the weak assumption that the overlap to continuum $A-1$ states is of shorter range than the overlap to the bound $A-1$ states [35], as is indeed the case for the present model.

This also means that the DWIA (distorted wave impulse approximation) analysis of $(e, e'p)$ reactions, strictly speaking, has a problem beyond the $A-1$ continuum threshold. Conventionally [31], one divides the missing energy range in bins and fits the (distorted) momentum distribution in each bin with an incoherent sum of DWIA momentum distributions corresponding to the relevant shell-model quantum numbers. The overlap functions entering the DWIA analysis are usually of the Woods-Saxon type, with the depth of the potential tuned so as to generate a bound state with single-particle energy equal to the separation energy of the bin. Such a procedure, inspired by the standard behavior (23), is for the continuum states clearly at variance with the results of the present exactly solvable model.

Nevertheless, the multipole decomposition of the $(e, e'p)$ continuum has always given quite plausible and consistent results. This may be due to the fact that, for fixed quantum numbers, one has kept the rms radius of the overlap function constant for different energy bins. The rms radius of the phenomenological bound-state wave function determines to a large extent its content in momentum space. Keeping the radius fixed would therefore help to ensure that similar momentum distributions are used for single-particle transitions in different energy bins in the continuum but belonging to the same channel, in agreement with the present model which leads to the same exponential decay for these overlap functions. An improved analysis of $(e, e'p)$ reactions in the $A-1$ continuum would in addition take into account the oscillatory behavior of the overlap functions related to the excess energy beyond the channel threshold. This seems to require the introduction of an imaginary part in the phenomenological single-particle potential, which is plausible since the physical self-energy in the $A-1$ continuum does have an imaginary part. Note that an imaginary part of the potential leads to damping for scattering solutions ($E > 0$), but would likewise introduce an oscillatory behavior for bound solutions ($E < 0$).

B. Distribution of single-particle strength

The removal spectral function is generally defined, in terms of the overlap functions of Eq. (19), as

$$S(x, x'; E) = \sum_{\nu(A-1)} \delta(E - E_{\nu(A-1)})\psi_{\nu(A-1)}(x)\psi^*_{\nu(A-1)}(x'). \tag{26}$$

For the present model, the summation in Eq. (26) can be split up as $S = S_Q + S_C$, and includes the contribution from the bound $A-1$ ground state (corresponding to the single cluster $[A-1]$ and henceforth called the quasihole contribution),

$$S_Q(x, x'; E) = \delta(E - E_{0(A-1)})\psi_{[A-1]}(x)\psi^*_{[A-1]}(x'), \tag{27}$$

as well as the contributions from the $(A-1)$ continuum channels, labeled by the other partitions $[P]$ of $A-1$,

$$\begin{aligned} &S_C(x, x'; E) \\ &= \sum_{[P]} \frac{1}{D_{[P]}} \int d\mathbf{K} \delta(E - E_{[P]\mathbf{K}})\psi_{[P]\mathbf{K}}(x)\psi^*_{[P]\mathbf{K}}(x') \\ &= \sum_{[P]} \frac{1}{D_{[P]}} \int_0^{+\infty} dK\, \delta\Big(E - E^{\mathrm{tr}}_{[P]} - K^2/(2m)\Big) F_{[P]}(x, x'; K). \end{aligned} \tag{28}$$

Note that at a fixed energy E only the open channels with threshold below E contribute. It was also convenient in Eq. (28) to introduce the variable K as $K^2/(2m) = E_{[P]\mathbf{K}} - E^{\mathrm{tr}}_{[P]}$, and

$$F_{[P]}(x, x'; K) = K^{N-2} \frac{1}{D_{[P]}} \int d\Omega\, \psi_{[P]\mathbf{K}}(x)\psi^*_{[P]\mathbf{K}}(x'), \tag{29}$$

where the integration is over the remaining $N-2$ angles specifying the relative momenta $\mathbf{K}$. An alternative expression

TABLE II. Total removal strength from the A-particle ground state, classified according to the different partitions of $A-1$, for $A=3,4,5$.

$A=3$	[2] 2.8148	$[1^2]$ 0.1851			
$A=4$	[3] 3.7620	[21] 0.2260	$[1^3]$ 0.0120		
$A=5$	[4] 4.7369	[31] 0.2301	$[21^2]$ 0.0156	$[2^2]$ 0.0167	$[1^4]$ 0.0007

for the correlation spectral function therefore reads

$$S_C(x,x';E)=\sum_{[P]}\theta\big(E-E^{\rm tr}_{[P]}\big)\frac{1}{K}F_{[P]}(x,x';K), \quad (30)$$

where $K=\sqrt{2m(E-E^{\rm tr}_{[P]})}$.

The well-known particle-number sum rule,

$$A=\int dE\int dx S(x,x;E)=\int dE S(E) \quad (31)$$

likewise picks up contributions from both the quasihole and the various continuum channels. In Table II we have listed, for $A=3,4,5$, the contribution of each partition $[P]$ to the sum rule (31). The quasihole state clearly carries the bulk of the strength. In a noninteracting boson system it would exhaust the sum rule completely; the nonzero strength residing in the other channels is a measure of the amount of correlations in the interacting system. The present system is only weakly correlated, as only about 5% of the strength is outside the quasihole state. The dominant correlation channel is the $[A-2,1]$ partition (roughly corresponding to the two-hole one-particle states in a fermionic system). Nevertheless, even the total breakup channel $[1^{A-1}]$ has nonvanishing single-particle strength.

In order to investigate in more detail the single-particle continuum strength we have shown in Fig. 1, for $A=5$, the contributions to the energy distribution

$$F_{[P]}(K)=\int dx F_{[P]}(x,x;K), \quad (32)$$

of the different channels. Note that $F_{[P]}(K)$ is plotted, rather than $S(E)$ which has an integrable singularity for the [31] channel at threshold. It is seen from Fig. 1 that the [31] channel dominates the continuum strength at all energies. Asymptotically, the energy distributions have a power-law tail where the power seems to be governed by the smallest cluster in the partition: it is identical for the [31], $[21^2]$, and $[1^4]$ partition, whereas the $[2^2]$ decays faster.

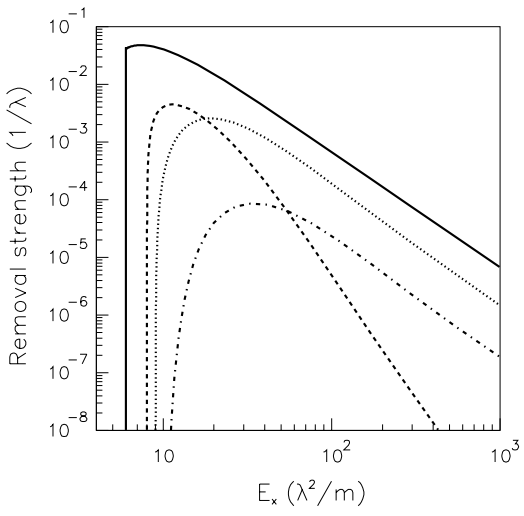

FIG. 1. Removal strength $F_{[P]}(K)$ as a function of excitation energy in the $(A-1)$-particle system, $E_x=K^2/(2m)+E^{\rm tr}_{[P]}-E_{[A-1]}$, for $A=5$ and the various continuum channels with partition labels [31] (solid line), $[2^2]$ (dashed line), $[21^2]$ (dotted line), $[1^4]$ (dash-dotted line).

C. Density and momentum distribution

The make up of the total density

$$\rho(x)=\int dE\ S(x,x;E) \quad (33)$$

is presented in Fig. 2. As shown already in Ref. [17], the density of the system is asymptotically dominated by the quasihole contribution, whereas the correlation contribution is more localized in the center and has a faster decay. The present work allows to separate the correlation contribution into its different continuum channel components. The exponential decay length for a certain partition $[P]$ is (in accordance with the results of Sec. III A) governed by the largest cluster present in $[P]$. The total break-up channel $[1^4]$ therefore has the fastest decay.

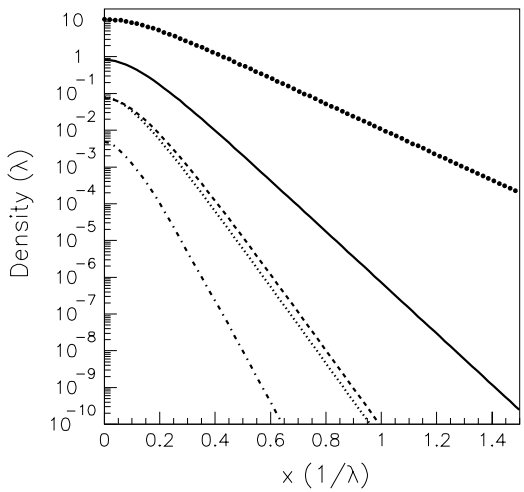

FIG. 2. Contributions to the density $\rho(x)$ for $A=5$, from the quasihole state (bullets) and from the various continuum channels (see caption of Fig. 1).

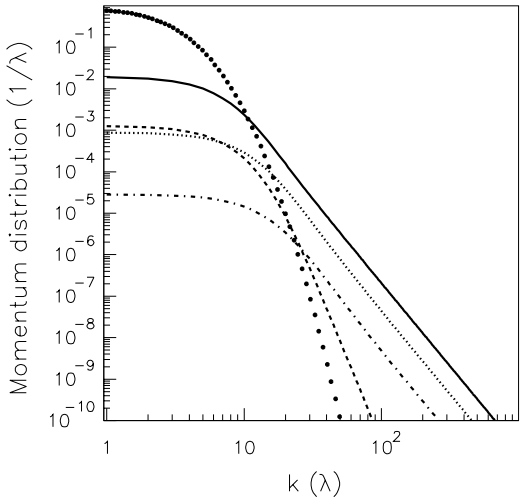

FIG. 3. Contributions to the momentum distribution $n(k)$ for $A = 5$, from the quasihole state (bullets) and from the various continuum channels (see caption of Fig. 1).

In Fig. 3 the momentum distribution of the system

$$n(k) = \int dE\ S(k;E) = \int dE \frac{1}{2\pi} \int dx \int dx' e^{ik(x-x')} S(x,x';E) \qquad (34)$$

is displayed in the same manner. As expected, the quasihole component dominates at small values of the momentum k, whereas the continuum channels determine the large-momentum region of the momentum distribution. Note that the [31] channel dominates the continuum contribution for all momenta, and that the asymptotic behavior of the various components of $n(k)$ is the same as those of the energy distribution $S(E)$ (i.e., power-law tails determined by the lightest cluster in $[P]$).

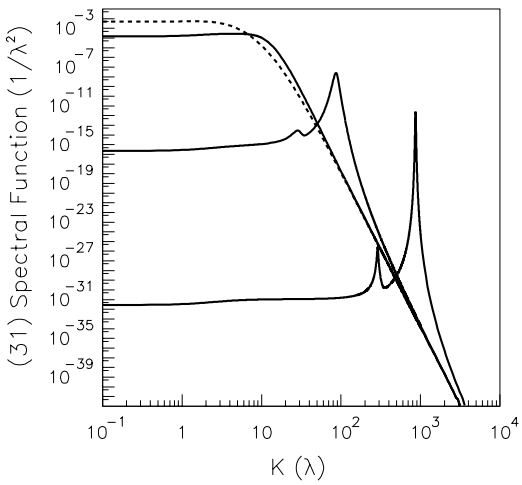

FIG. 4. For $A = 5$, the spectral strength $F_{[31]}(k;K)$ as a function of K, for momentum $k = 0$ (dashed line) and for $k = 10, 100, 1000$ λ (solid lines, with a larger k corresponding to a maximum at larger K).

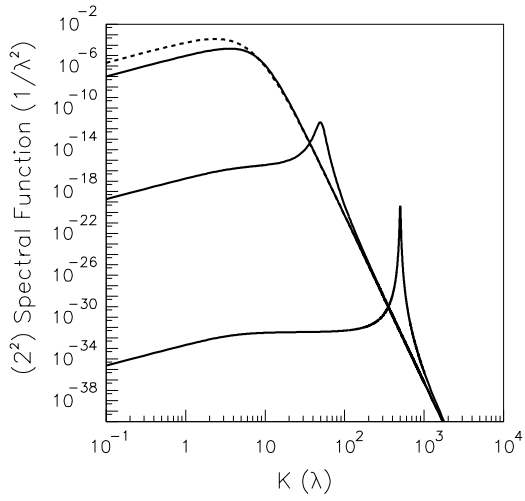

FIG. 5. Same as Fig. 4, for the spectral strength $F_{[2^2]}(k;K)$.

D. Correlation ridges

The identical behavior of $S(E)$ and $n(k)$ at large values of E and k can be understood from the structure of the momentum-space spectral function

$$S(k;E) = \sum_{[P]} \theta\left(E - E^{\rm tr}_{[P]}\right) \frac{1}{K} F_{[P]}(k;K). \qquad (35)$$

The functions $F_{[P]}(k;K)$ for the various partitions are presented in Figs. 4–7, and are plotted as a function of K for fixed $k = 0, 10, 100, 1000$ λ. In each partition, the spectral strength is for larger k increasingly dominated by a single peak at a value $K_{\rm max} = \alpha k$ with $\alpha = \sqrt{3/4}$ for [31], $[21^2]$, $[1^4]$ and $\alpha = \sqrt{1/2}$ for $[2^2]$. This reflects the most favorable configuration, where the large external momentum k is counterbalanced by the momentum of the lightest cluster available. In general, for a partition $[P]$ of $A - 1$ with a lightest cluster of n particles

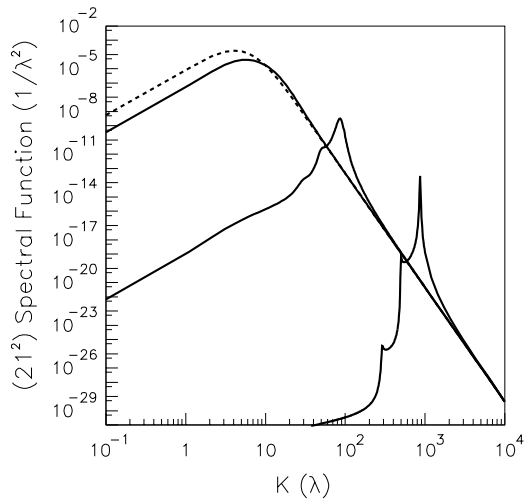

FIG. 6. Same as Fig. 4, for the spectral strength $F_{[21^2]}(k;K)$.

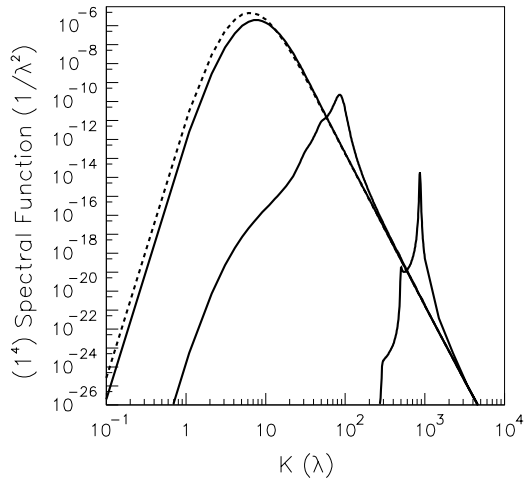

FIG. 7. Same as Fig. 4, for the spectral strength $F_{[1^4]}(k; K)$.

one finds by straightforward reasoning that

$$K_{\max} = \sqrt{\frac{A-n-1}{n(A-1)}}\lambda. \tag{36}$$

In Fig. 8 the location $K_{\max}$ of the maximum of $F_{[P]}(k, K)$ has been plotted, as a function of k. Figure 9 contains the corresponding strength $F_{[P]}(k, K_{\max})$. For large k and E virtually all the strength is concentrated along these correlation ridges. The integrated quantities $S(E)$ or $n(k)$ pick up almost exclusively the peak strength, and therefore contain essentially the same information. It is clear from Fig. 5 that the most important correlation ridge is the one associated with the $[A-2, 1]$ partition. This amounts to the well-known process in which a high-momentum particle is removed from the small component in the A-particle ground-state consisting of a correlated pair on top of the $A-2$ ground state.

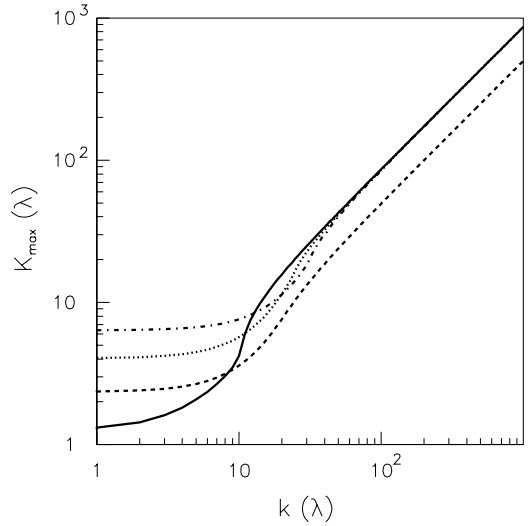

FIG. 8. For $A = 5$, the position $K_{\max}$ of the maximum of the spectral strength $F_{[P]}(k; K)$, as a function of k and for the various continuum channels (see caption of Fig. 1).

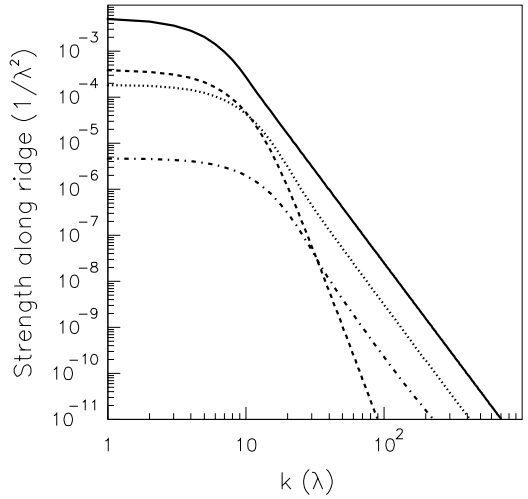

FIG. 9. For $A = 5$, the value $F_{[P]}(k; K_{\max})$ at the maximum, as a function of k and for the various continuum channels (see caption of Fig. 1).

Another interesting observation, clearly visible from Figs. 4–7, is that for each continuum channel the removal spectral function at large energy eventually reaches a universal power-law tail, irrespective of the value of k. Such a behavior indicates a regime purely driven by the available phase space. The background distribution coincides with the large-energy part of the $k = 0$ spectral function and is shown in Fig. 10 for the various partitions. Note that the tail is proportional for the [31] and $[2^2]$, and for the $[21^2]$ and $[1^4]$ partition. The presence of a common tail at large removal energies, for the exact spectral function in the present model, is a feature that is also found in recent nuclear-matter calculations using the framework of self-consistent Green function theory [32,33]. Since the removal spectral function contributes to the binding energy, this is an important property reproduced in a

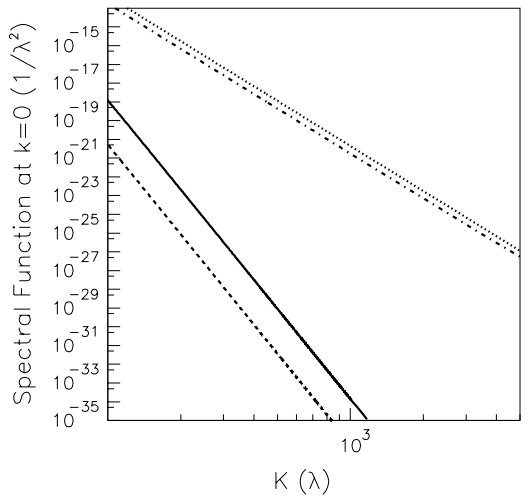

FIG. 10. For $A = 5$, the large-energy behavior of $F_{[P]}(k = 0; K)$ for the various continuum channels (see caption of Fig. 1).

self-consistent approach, but lacking in calculations where the self-energy is evaluated using mean-field propagators.

IV. SUMMARY AND CONCLUSIONS

We have investigated a model of one-dimensional bosons interacting with attractive delta potentials. As the model is exacly solvable, it can be used to elucidate the structure of single-particle overlap functions with unbound $A-1$ states, and to look at some of their exact properties without the usual uncertainties introduced by approximate many-body methods. It seems, e.g., that a commonly assumed large-distance behavior does not hold for the overlap with unbound $A-1$ states, a fact that may be relevant for the analysis of $(e, e' p)$ reactions with the final state of the residual nucleus in the continuum.

While the most important continuum contribution is the one associated with a bound $A-2$ state and a single particle in the continuum, other break-up channels of the $A-1$ system also contribute to the removal strength, and hence to the density and the momentum distribution.

At large values of energy and momentum the continuum strength is concentrated along correlation ridges which completely dominate the spectral function. The position of these ridges is determined by the lightest cluster in the asymptotic partition of the $A-1$ system, and is easily understood by kinematical arguments.

Finally, for any fixed value of the single-particle momentum k, the large-energy behavior of the spectral function is universal and does not depend on k.

ACKNOWLEDGMENT

This work is supported by the Fund for Scientific Research-Flanders (FWO-Vlaanderen) and the Research Council of Ghent University.

APPENDIX

The cusp conditions (5) imply that if an exponential term $\exp(\sum_{i=1}^{A} e_i x_i)$ is present in $\Psi_{(A)}^{\mathrm{SO}}$ then, unless special constraints are imposed on the e_i, all permuted terms $\exp(\sum_{i=1}^{A} e_{\pi(i)} x_i)$ must also be present. The general exponential-type wave function that satisfies this requirement, for an arbitrary set of complex $e_i, i = 1, \ldots A$, is given in Eq. (6). The coefficients W_π are to be determined from the cusp conditions (5), which for the standard ordering can be restricted to the boundaries $x_k = x_{k+1}$ (with $k = 1, \ldots, A-1$), and read

$$\sum_{\pi} [2\lambda + e_{\pi(k)} - e_{\pi(k+1)}] \times \exp\left((e_{\pi(k)} + e_{\pi(k+1)}) x_k + \sum_{i \neq k, k+1} e_{\pi(i)} x_i \right) = 0. \quad \text{(A1)}$$

Denoted by t_k the transposition $k \leftrightarrow k+1$, each permutation π has a unique partner $\pi' = \pi t_k$ for which $\sum_{i=1}^{A} e_{\pi(i)} x_i = \sum_{i=1}^{A} e_{\pi'(i)} x_i$ at the boundary $x_k = x_{k+1}$. The cusp conditions for the wave function (6) therefore become

$$W_\pi [2\lambda + e_{\pi(k)} - e_{\pi(k+1)}] + W_{\pi t_k} [2\lambda - e_{\pi(k)} + e_{\pi(k+1)}] = 0, \quad \text{(A2)}$$

for all permutations π and all $k = 1, \ldots, A-1$.

A solution to the set of equations (A2) is easily seen to be

$$W_\pi = \mathrm{sign}(\pi) \prod_{i<j=1}^{A} [2\lambda - e_{\pi(i)} + e_{\pi(j)}], \quad \text{(A3)}$$

by noting that

$$W_{\pi t_k} = -W_\pi \frac{2\lambda + e_{\pi(k)} - e_{\pi(k+1)}}{2\lambda - e_{\pi(k)} + e_{\pi(k+1)}}. \quad \text{(A4)}$$

This shows that a wave function $\Psi_{(A)}^{\mathrm{SO}}$ of the form (6), with coefficients W_π given by Eq. (A3), is an eigenfunction of the Hamiltonian H_A for an arbitrary choice of the e_i.

[1] A. L. Fetter and J. D. Walecka, *Quantum Theory of Many-Particle Systems* (McGraw-Hill, San Francisco, 1971).
[2] W. H. Dickhoff and D. Van Neck, *Many-Body Theory Exposed!* (World Scientific, Singapore, 2005).
[3] A. E. L. Dieperink and P. K. A. deWitt-Huberts, Annu. Rev. Nucl. Part. Sci. **40**, 239 (1990).
[4] L. Lapikás, Nucl. Phys. **A553**, 297c (1993).
[5] V. R. Pandharipande, I. Sick, and P. K. A. deWitt-Huberts, Rev. Mod. Phys. **69**, 981 (1997).
[6] D. Rohe, Eur. Phys. J. A **17**, 493 (2003).
[7] D. Rohe *et al.*, Phys. Rev. Lett. **93**, 182501 (2004).
[8] M. van Batenburg, Ph.D. thesis, University of Utrecht, 2001.
[9] H. Müther and W. H. Dickhoff, Phys. Rev. C **49**, R17 (1994).
[10] O. Benhar, C. Ciofi degli Atti, S. Liuti, and G. Salmé, Phys. Lett. **B177**, 135 (1986).
[11] O. Benhar, A. Fabrocini, S. Fantoni, and I. Sick, Nucl. Phys. **A579**, 493 (1994); I. Sick, S. Fantoni, A. Fabrocini, and O. Benhar, Phys. Lett. **B323**, 267 (1994).
[12] D. Van Neck, A. E. L. Dieperink, and E. Moya de Guerra, Phys. Rev. C **51**, 1800 (1995).
[13] H. Müther, A. Polls, and W. H. Dickhoff, Phys. Rev. C **51**, 3040 (1995).
[14] F. Calogero and A. Degasperis, Phys. Rev. A **11**, 265 (1975).
[15] R. D. Amado, Phys. Rev. C **14**, 1264 (1976); R. D. Amado and R. M. Woloshyn, Phys. Lett. **B62**, 253 (1976).
[16] R. D. Amado and R. M. Woloshyn, Phys. Rev. C **15**, 2200 (1977).
[17] D. Van Neck, A. E. L. Dieperink, and M. Waroquier, Phys. Rev. C **53**, 2231 (1996).
[18] D. Van Neck, A. E. L. Dieperink, and M. Waroquier, Z. Phys. A **355**, 107 (1996).
[19] D. Van Neck, L. Van Daele, Y. Dewulf, and M. Waroquier, Phys. Rev. C **56**, 1398 (1997).
[20] M. V. Stoitsov, S. S. Dimitrova, and A. N. Antonov, Phys. Rev. C **53**, 1254 (1996); S. S. Dimitrova, M. K. Gaidarov, A. N. Antonov, M. V. Stoitsov, P. E. Hodgson, V. K. Lukyanov, E. V. Zemlyanaya, and G. Z. Krumova, J. Phys. G: Nucl. Part. Phys. **23**, 1685 (1997); M. K. Gaidarov, K. A. Pavlova, S. S. Dimitrova, M. V. Stoitsov, A. N. Antonov, D. Van Neck, and H. Müther, Phys. Rev. C **60**, 024312 (1999); M. K. Gaidarov, K. A. Pavlova, A. N. Antonov, M. V. Stoitsov, S. S. Dimitrova,

M. V. Ivanov, and C. Giusti, *ibid.* **61**, 014306 (2000); M. K. Gaidarov, K. A. Pavlova, A. N. Antonov, C. Giusti, S. E. Massen, C. C. Moustakidis, and K. Spasova, *ibid.* **66**, 064308 (2002).
[21] A. Fabrocini and G. Co', Phys. Rev. C **63**, 044319 (2001).
[22] A. Polls, H. Müther, and W. H. Dickhoff, Nucl. Phys. **A594**, 117 (1995).
[23] H. Müther and I. Sick, Phys. Rev. C **70**, 041301(R) (2004).
[24] L. Lapikas, G. van der Steenhoven, L. Frankfurt, M. Strikman, and M. Zhalov, Phys. Rev. C **61**, 064325 (2000).
[25] Y. Castin and C. Herzog, C. R. Acad. Sci. Paris S'erie **4**, 419 (2001).
[26] D. Van Neck and M. Waroquier, Phys. Rev. C **58**, 3359 (1998).
[27] E. H. Lieb and W. Liniger, Phys. Rev. **130**, 1605 (1963).
[28] C. Mahaux and R. Sartor, Advances in Nuclear Physics **20**, 1 (1991).
[29] J. M. Bang, F. G. Gareev, W. T. Pinkston, and J. S. Vaagen, Phys. Rep. **125**, 253 (1985).
[30] D. Van Neck, M. Waroquier, and K. Heyde, Phys. Lett. **B314**, 255 (1993).
[31] J. J. Kelly, Advances in Nuclear Physics **23**, 75 (1996).
[32] W. H. Dickhoff and E. P. Roth, Acta Phys. Pol. B **33**, 65 (2002).
[33] Y. Dewulf, D. Van Neck, and M. Waroquier, Phys. Rev. C **65**, 054316 (2002).
[34] The factor $(A-1)/A$ reflects the reduced mass in the present self-bound system and is not present for a fixed-center system.
[35] We would like to thank the referee of Ref. [30] for pointing this out.